Journal of Reproduction and Development, Vol. 67, No 6, 2021

Original Article

Neuronal activation modulates enhancer activity of genes for excitatory synaptogenesis through *de novo* DNA methylation

Tomonori KAMEDA[1, 2], Hideyuki NAKASHIMA[1], Takumi TAKIZAWA[3], Fumihito MIURA[4], Takashi ITO[4], Kinichi NAKASHIMA[1] and Takuya IMAMURA[1, 2]

[1]*Department of Stem Cell Biology and Medicine, Graduate School of Medical Sciences, Kyushu University, Fukuoka 812-8582, Japan*
[2]*Laboratory of Molecular and Cellular Physiology, Graduate School of Integrated Sciences for Life, Hiroshima University, Hiroshima 739-8526, Japan*
[3]*Department of Pediatrics, Graduate School of Medicine, Gunma University, Gunma 371-8511, Japan*
[4]*Department of Biochemistry, Graduate School of Medical Sciences, Kyushu University, Fukuoka 812-8582, Japan*

Abstract. Post-mitotic neurons do exhibit DNA methylation changes, contrary to the longstanding belief that the epigenetic pattern in terminally differentiated cells is essentially unchanged. While the mechanism and physiological significance of DNA demethylation in neurons have been extensively elucidated, the occurrence of *de novo* DNA methylation and its impacts have been much less investigated. In the present study, we showed that neuronal activation induces *de novo* DNA methylation at enhancer regions, which can repress target genes in primary cultured hippocampal neurons. The functional significance of this *de novo* DNA methylation was underpinned by the demonstration that inhibition of DNA methyltransferase (DNMT) activity decreased neuronal activity-induced excitatory synaptogenesis. Overexpression of WW and C2 domain-containing 1 (*Wwc1*), a representative target gene of *de novo* DNA methylation, could phenocopy this DNMT inhibition-induced decrease in synaptogenesis. We found that both DNMT1 and DNMT3a were required for neuronal activity-induced *de novo* DNA methylation of the *Wwc1* enhancer. Taken together, we concluded that neuronal activity-induced *de novo* DNA methylation that affects gene expression has an impact on neuronal physiology that is comparable to that of DNA demethylation. Since the different requirements of DNMTs for germ cell and embryonic development are known, our findings also have considerable implications for future studies on epigenomics in the field of reproductive biology.
Key words: *De novo* DNA methylation, Enhancer regulation, Synapse formation

(**J. Reprod. Dev. 67:** 369–379, 2021)

DNA methylation is catalyzed by DNA methyltransferases (DNMTs) and occurs most frequently at cytosines in CpG dinucleotides [1, 2]. During cell differentiation, the DNA methylation pattern defines transcription in a highly cell type- and genomic context-dependent manner [3, 4]. Genome-wide studies during brain development have revealed large-scale changes in the DNA methylation status, especially in DNA demethylation [5]. Interestingly, in neurons, DNA demethylation can be observed even at the post-mitotic stages, raising the possibility that dynamic DNA methylation changes could functionally contribute to neuronal physiology, such as spine formation or synaptic transmission [6, 7]. Indeed, the notion that genomic DNA methylation in differentiated cells is mostly irreversible has been overturned by several reports on the loss of DNA methylation in post-mitotic neurons [8–13]. Emerging evidence has shown the critical roles of epigenetic modifications, including DNA methylation changes, in the regulation of neuronal plasticity, learning, and memory formation [7, 10, 14–18]. In association with DNA demethylation, histone modification, especially histone acetylation, which results in the relaxation of chromatin in general, contributes to enhanced transcription of memory-related genes [19, 20]. In response to neuronal activation, there is marked induction of histone acetylation along with enhancer RNA or DNA demethylation at some promoter and enhancer regions [7, 21–23].

De novo DNA methylation also occurs in a neuronal activity-dependent manner, and uncovering its functional roles, if there are any, would greatly strengthen the idea that dynamic DNA methylation has considerable impacts on neuronal physiology, because changing in a bidirectional way rather than unidirectional loss of DNA methylation would enable more complex phenotypic expression. In fact, among the different DNMTs, DNMT1 and DNMT3a are abundant in post-mitotic neurons [24, 25]. Several lines of evidence have suggested that epigenetic changes, such as *de novo* DNA methylation, suppress gene expression in a neuronal activity-dependent manner [9]. For example, experience induces *de novo* DNA methylation in the CA1 area of the hippocampus, and these DNA methylation changes have been observed in memory-related genes [9, 18]. Furthermore, pharmacological inhibition of DNMT activity or double knockout of *Dnmt1* and *Dnmt3a* disrupts the memory function in adult rodents [9, 17, 26]. The contribution of DNMT3a to *de novo* DNA methylation is widely accepted because it methylates cytosines at previously unmethylated CpG sites on a single DNA strand, and is thus called *de novo* DNMT. In the context of germ cell and zygotic development, DNMT3b and DNMT3l have been shown to be involved in these processes, in addition to DNMT3a. For example, DNMT3l is an epigenetic modifier that is closely associated with transcriptional repression

Received: August 22, 2021
Accepted: September 11, 2021
Advanced Epub: October 7, 2021

Correspondence: T Imamura (e-mail: timamura@hiroshima-u.ac.jp),
K Nakashima (e-mail: kin1@scb.med.kyushu-u.ac.jp)

and is crucial for genome-wide reprogramming in embryonic germ cells [27–29]. DNMT3l itself does not possess enzymatic activity but acts to promote *de novo* methylation of DNA sequences, including retrotransposons, gene bodies, and the regulatory sequences of imprinted genes [30–34]. In contrast, DNMT1 recognizes methylated CpG sites on a single strand and subsequently methylates cytosines on the opposite strand, and is thus called a maintenance DNMT [24, 25]. Nevertheless, DNMT1 also exhibits considerable *de novo* DNA methylase activity [35, 36]. Therefore, the involvement of DNMT1 in *de novo* DNA methylation has not been ruled out in the context of neuronal maturation during development, even if preventing aberrant *de novo* DNA methylation mediated by DNMT1 safeguards the unique oocyte epigenome [37].

DNA methylation is a crucial topic in reproductive biology. It plays important roles in the formation, proliferation, and differentiation of multipotent stem cells. On the other hand, post-mitotic neurons are non-proliferative and terminally differentiated cells, and thus, neurons are well-suited for the study of active DNA methylation changes, if any. In this study, we investigated neuronal activity-dependent DNA methylation changes at single-base resolution in primary cultured mouse hippocampal neurons. We found that neuronal activation induced both *de novo* DNA methylation and DNA demethylation at comparable levels, mainly in genomic regions that could be annotated as enhancers. RNA-seq data and experiments evaluating the enhancer activity of a representative *de novo* DNA-methylated region supported the idea that neuronal activity-dependent *de novo* DNA methylation could downregulate target gene expression by suppressing enhancer activity. In the present study, we provide evidence that DNMT1 and/or DNMT3a are involved in the observed neuronal activity-induced *de novo* DNA methylation during synaptogenesis.

Materials and Methods

Animals

All aspects of animal care and treatment were performed according to the guidelines of the Experimental Animal Care Committee of Kyushu University (Fukuoka, Japan). Timed-pregnant ICR mice (Japan SLC) and C57BL/6 mice [only for PBAT; Japan SLC] were used in this study.

Constructs

Lentivirus vectors used to express short-hairpin RNAs (shRNAs; pLLX) and FLAG-tagged MeCP2 (pLEMPRA) [38, 39] were provided by Dr. Z. Zhou (University of Pennsylvania School of Medicine, Philadelphia, PA, USA) and Dr. M. E. Greenberg (Harvard Medical School, Boston, MA, USA). A FLAG-tagged mouse WWC1 expression lentivirus vector was constructed by replacing MeCP2 with *Wwc1* at the *EcoRI* (Takara Bio, Shiga, Japan; catalog no. 1040A) and *AscI* (New England Biolabs, Ipswich, MA, USA; catalog no. R0558S) sites of pLEMPRA-MeCP2. shRNAs against *Wwc1*, *Dnmt1,* and *Dnmt3a* were designed to target mouse genes.

Cell culture

Hippocampal neurons were isolated from embryonic day (E) 17 mice (male and female), according to a previously described protocol [40]. Cytosine β-d-arabinofuranoside hydrochloride (Sigma-Aldrich, St. Louis, MO, USA; catalog no. 855855) was added 1 d after plating, to eliminate proliferating, undifferentiated, and glial cells. To inhibit DNMT activity, the neurons were treated with 100 µM RG108 (Wako, Tokyo, Japan; catalog no. 041-30101) overnight. To suppress spontaneous neuronal activation, the neurons were treated with 1 µM tetrodotoxin (Abcam, Cambridge, UK; catalog no. ab120055), from 1 to 10 DIV. To induce neuronal activation, 10 DIV neurons were treated with 50 µM bicuculline (Wako; catalog no. 026-16131) and 200 µM 4-aminopyridine (Sigma-Aldrich; catalog no. 275875) for 3 or 6 h. We confirmed the cell viability after neuronal activation by observing the rare presence of active caspase 3-positive cells (Supplementary Fig. 10). Lentiviruses were produced as described previously [41]. The virus was introduced into the neurons at 6 DIV.

Mouse neuroblastoma Neuro2a cells were cultured in DMEM (Nacalai Tesque, Kyoto, Japan; catalog no. 08458-45) supplemented with 10% FBS (Sigma-Aldrich; catalog no. F7524) and 20 µM retinoic acid (Sigma-Aldrich; catalog no. R2625).

Luciferase reporter assay

DNA fragments corresponding to hyperDMRs (*Wwc1, Dpf1, Kat6B,* and *Sergef* gene body) were inserted upstream of the hEF1 promoter in the pCpG-free promoter with the Lucia reporter gene (Invivogen, San Diego, CA, USA; catalog no. pcpgf-promlc) [23]. The pCpG-free promoter with the Lucia reporter gene was treated with CpG methyltransferase (M.SssI, New England Biolabs; catalog no. M0226) for 1 h at 37°C. Neuro2a cells treated with retinoic acid were transfected with a CpG-free reporter construct that harbored the *Wwc1* hyperDMR or an empty construct using PEI (Sigma-Aldrich; catalog no. 919012). After transfection, the cells were incubated for 2 d and 10 µl of the cell supernatant was mixed with 50 µl of QUANTI-Luc™ reagent (Invivogen; catalog no. rep-qlc1). E17 mouse hippocampal neurons were transfected with a CpG-free reporter construct that harbored the *Wwc1, Dpf1, Kat6B,* or *Sergef* hyperDMR or an empty construct using the Neon™ Transfection System (Invitrogen, Waltham, MA, USA; pulse voltage: 1500 V; pulse width: 10 ms; number of pulses: 3). After transfection, the cells were incubated for 1 day and 20 µl of the cell supernatant was mixed with 50 µl of QUANTI-Luc™ reagent. Lucia activity was determined in four independent transfections and measured using a luminometer (ARVO Light, PerkinElmer, Waltham, MA, USA).

qRT-PCR analysis

Total RNA was isolated with Sepasol-RNA I Super G (Nacalai Tesque; catalog no. 09379-55) and subjected to reverse transcription with the SuperScript™ VILO cDNA Synthesis Kit (Invitrogen; catalog no. 11754050), according to the manufacturer's instructions. qRT-PCR was performed using a KAPA SYBR® Fast qPCR Kit (Kapa Biosystems, Tokyo, Japan; catalog no. KK4600) with ROX as the reference dye using the StepOne™ Real-Time PCR System (Applied Biosystems, Waltham, MA, USA). The expression levels of each gene were normalized to GAPDH and calculated relative to that of the control.

RNA sequencing and data analysis

RNA sequencing was performed with 36-bp single-end sequencing using an Illumina Hiseq® 3000 system (Illumina, San Diego, CA, USA), as described previously [42]. The obtained reads were processed with the FASTX tool kit (Hannon Lab) [43] to remove short (< 20 bp) and low-quality (quality score < 20) reads, followed by trimming of the adaptor sequence. Processed reads were aligned to the genome assembly mm10 using TopHat (Trapnell lab) [44]. We used RPKM values to compare gene expression changes. To identify hyperDMR target genes, genes whose expression was less than 1 RPKM before neuronal activation (no treatment) were excluded.

ChIP-seq and data analysis

Chromatin immunoprecipitation (ChIP) was carried out using mouse monoclonal anti-H3K27ac (MBL, Aichi, Japan; catalog no. MABI0309) and anti-H3K4me1 (MBL; catalog no. MABI0302) antibodies, as previously described [45]. For each antibody, we obtained data from two independent samples, confirmed similar mapping patterns between the replicates, and merged these data for peak-calling, which was performed using MACS version 1.4.1 (https://pypi.org/project/MACS/) [46]. Genomic annotation of the peaks identified from the ChIP-seq data was performed using GREAT (http://great.stanford.edu/public/html/) [47]. Density profiles of chromatin marks around the hyperDMRs were computed with Ngsplot (Shen Lab) using the max option [48]. We used the other histone marks from GSE21161. We checked the previously reported *c-Fos* enhancer regions and validated our H3K27ac and H3K4me1 data (Supplementary Fig. 11).

WGBS and data analysis

Genomic DNA was subjected to bisulfite treatment using the EZ DNA Methylation-Gold™ Kit (ZYMO Research, Irvine, CA, USA; catalog no. D5005), according to the manufacturer's instructions. In this study, we adopted a strategy termed post-bisulfite adaptor tagging (PBAT), which provides unbiased methylome analysis [49, 50]. The multiplex PBAT method is also described in detail on the CREST/IHEC Japan webpage (http://crest-ihec.jp/english/epigenome/index.html). PBAT single-end reads were mapped to the mouse mm10 reference genome using BMap software (http://itolab.med.kyushu-u.ac.jp/BMap/index.html) [49] with default parameter settings. We utilized WGBS data composed of more than 0.5 billion reads, with 75% of CpG sites in the mouse genome covered by at least five reads. DMRs were defined according to a previously described protocol [5]. Hypo- or hyperDMRs were defined as > 4 DMS (methylation change ≥ 0.3), with a distance of less than 250 bp between adjacent DMS. Gene ontology (GO) analysis for DMR-associated genes was performed using Database for Annotation, Visualization and Integrated Discovery (DAVID) (https://david.ncifcrf.gov/) [51].

Bisulfite sequencing

To determine the DNA methylation profiles of the hyperDMR at the *Wwc1* gene body, genomic DNA from primary cultured hippocampal neurons was subjected to bisulfite reaction using a Methylamp kit (Epigentek, Farmingdale, NY, USA; catalog no. P-1001), according to the manufacturer's instructions. Each bisulfite-treated genome was amplified using AmpliTaq Gold™ 360 Master Mix (Life Technologies, Carlsbad, CA, USA; catalog no. 4398886) and specific primers. We performed bisulfite sequencing of more than 10 clones from each sample. Sequences were analyzed using the methylation analysis tool QUantification tool for Methylation Analysis (QUMA: http://quma.cdb.riken.jp/top/index.html). We excluded identical bisulfite sequences using the QUMA option. The statistical significance of differences between the two groups of the entire set of CpG sites was evaluated using the Wilcoxon rank-sum test (also called the Mann–Whitney *U*-test).

Quantification and statistical analysis

No statistical methods were used to determine the sample sizes. Data points were not excluded from the analysis. We did not use any methods to determine whether the data met the assumptions of the statistical approach. All data were collected and processed randomly. Statistical analyses were performed using a sample size of 3 or 4. Unpaired Student's *t*-tests (for quantifying gene expression and synapse density) and the Wilcoxon rank-sum test (for quantifying DNA methylation level using bisulfite sequencing) were used to calculate the *p*-value for pairwise comparisons. For multiple comparisons, *p*-values were calculated using Tukey's multiple comparison test (for gene expression and luciferase reporter assay) and Wilcoxon rank-sum test (for boxplot of gene expression or methylation level at DMRs from NGS data). The exact values of n (sample size) are provided in the figure legends. Statistical significance was set at *p*-value less than 0.05. Data have been represented as mean ± SEM.

Results

Neuronal activation induced global de novo DNA methylation, as well as, DNA demethylation

To examine DNA methylation changes upon neuronal stimulation, we conducted DNA methylome analysis using the post-bisulfite adapter-tagging method in primary cultured mouse hippocampal neurons that were treated with either TTX to suppress spontaneous neuronal activity or for 3 h with bicuculline/4-aminopyridine (Bic/4AP) to induce neuronal activation. The sequencing summary is shown in Additional File 1: Supplementary Table 1. When we identified DMS candidates in our previous study [13] [DMS candidate: 0.3 ≥ methylated (hyper) or demethylated (hypo) CpG sites, when compared between TTX- and Bic/4AP-treated samples], we found that both *de novo* DNA methylation and demethylation at CpG sites, predominant targets for DNA methylation, occurred in a genome-wide manner following neuronal activation (Supplementary Fig. 1A-B: ~4.5% CpGs in total were targeted). Based on the information on hypo- or hyperDMS candidates, we defined differentially methylated regions (DMRs) as regions that contained more than four DMS candidates, with a distance of less than 250 bp between adjacent DMS candidates (see *Materials and Methods*) and identified 826 Bic/4AP-dependent hyperDMRs and 1,075 hypoDMRs (Fig. 1B). To test if the bias in the presence of hypo- and hyperDMRs could be seen at the DMR level, we mapped DMRs along the chromosomes. We found that there was no significant bias in the presence of hypo- and hyperDMRs in the sex chromosomes (Fig. 1A). As shown in Fig. 1B, the defined hypo- and hyperDMRs were clearly segregated in the genome. DNA methylation changes at each DMR seemed to depend largely on the neuronal activity level, because genome-wide analysis showed that the methylation level at both hyperDMRs and hypoDMRs in the untreated sample exhibited median values between those for TTX- and Bic/4AP-treated samples (Fig. 1C-D). It is well known that CpG methylation is prevalent and non-CpG methylation occurs rarely in mammals. We also detected rare occurrences of non-CpG (CpH) methylation and demethylation upon neuronal activation (Supplementary Fig. 2A-B: ~0.15% of CpHs in total were targeted). There was a tendency of a positive correlation between CpG methylation changes and CpH methylation changes, although we could not detect a statistically significant effect (Supplementary Fig. 2C). These results clearly indicated that neuronal activation induced both global *de novo* DNA methylation and demethylation.

Neuronal activity-induced de novo DNA methylation at enhancer regions inversely correlated with gene expression independent of histone acetylation

It has been reported that the *Bdnf* promoter is demethylated by neuronal activation through the upregulation of *Tet3*, an enzyme involved in an active DNA demethylation pathway, and this demethylation regulates synaptic transmission [7]. Indeed, our data confirmed the neuronal activity-dependent DNA demethylation at the *Bdnf*

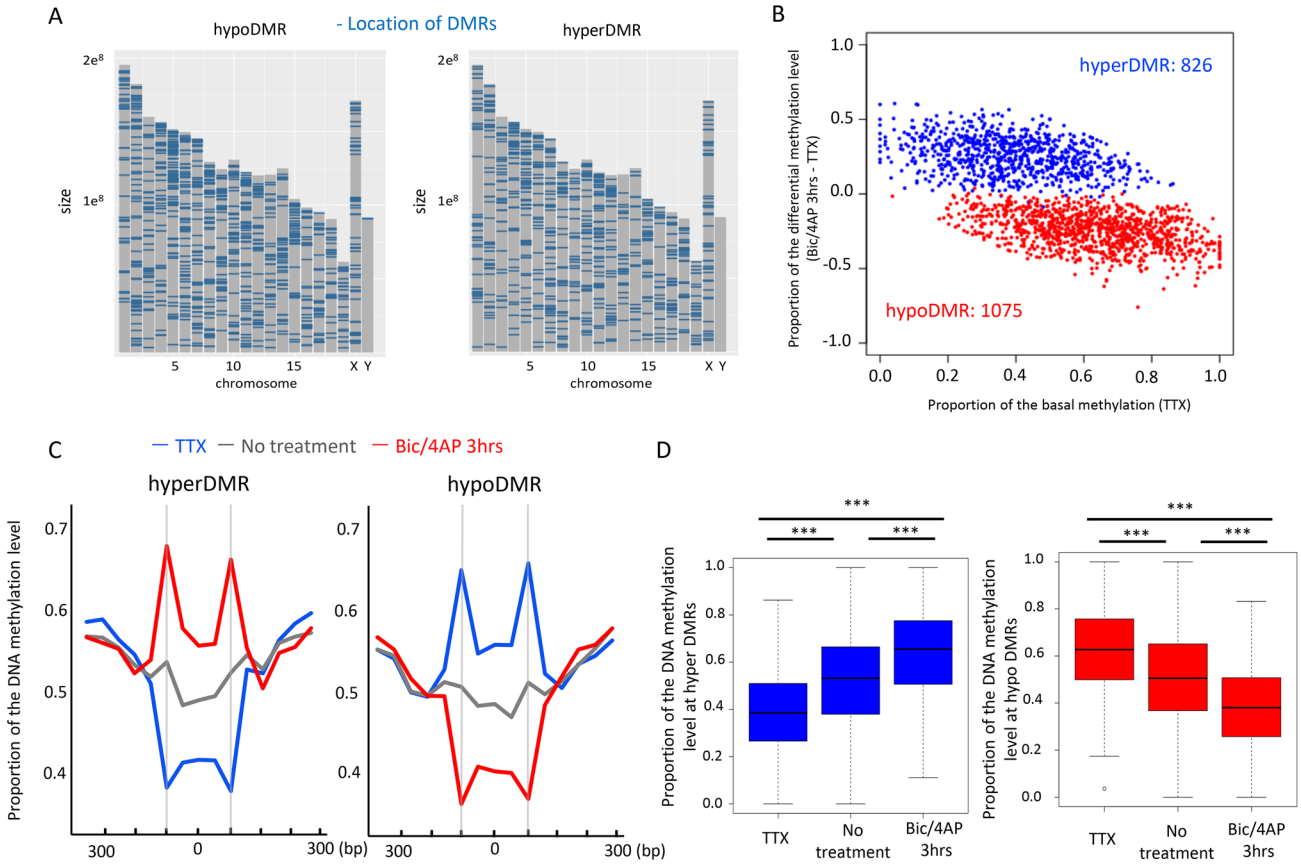

Fig. 1. Dynamics of neuronal activity-dependent DNA methylation. (A) Plot of genomic location of hypo- (left) and hyper- (right) DMRs across all the chromosomes. (B) Number of DMRs identified by comparison of samples treated with TTX and with Bic/4AP (for 3 h) and scatter plot of differences in DNA methylation patterns at each DMR. (C) Methylation-level patterns per 50 bp around hyperDMRs and hypoDMRs. All DMRs were standardized and plotted in terms of average length. The center of the DMR was set to 0 as the reference point for the plot. (D) Box plot of DNA methylation level at hyperDMRs and hypoDMRs. $P < 2.2e^{-16}$, Mann–Whitney U test.

promoter (Supplementary Fig. 3). We then focused on characterizing the target distribution of activity-induced *de novo* DNA methylation in the whole genome. We used the GREAT software to calculate the positions of hyperDMRs in relation to the transcription start sites. We found that hyperDMRs were mainly (over 80%) distributed more than 5 kb distal to the transcription start sites (Fig. 2A). The genomic locations of DMRs in relation to the gene structure are shown in Fig. 2B. Hyper- and hypoDMRs appeared to be enriched in the gene bodies (Fig. 2B, Supplementary Fig. 1B, and Supplementary Fig. 3B). Using publicly available ChIP-seq data of histone modifications [7 days *in vitro* cultured (DIV) cortical neurons; GSE21161], we found that H3K4me1 was highly accumulated at the hyperDMRs, as compared to either H3K4me3 or H3K27me3 (Supplementary Fig. 4). We also performed H3K4me1 ChIP-seq for our samples corresponding to 10 DIV hippocampal neurons. We confirmed that H3K4me1 accumulated in the hyperDMRs (Fig. 2C-D). Since H3K4me1 is known to accumulate in enhancer regions, these data suggested that neuronal activity-dependent DNA methylation changes may occur at candidate enhancer regions. We investigated the change in H3K27ac at DMRs because dynamic fluctuations of H3K27ac in the enhancer regions have been reported in a neuronal activity-dependent manner [21, 22]. Surprisingly, in contrast to significant DNA methylation at hyperDMR, alterations in H3K27ac upon neuronal stimulation were barely observed (Fig. 2E) when compared between the untreated sample (control) and the Bic/4AP-treated sample, suggesting that neuronal activity-dependent *de novo* DNA methylation occurs irrespective of histone acetylation. We further examined chromatin accessibility using ATAC sequencing of adult mouse dentate gyrus, before and after synchronous neuronal activation *via* electroconvulsive stimulation (GEO accession number: GSE82015) [52], and only a slight increase was observed in hyperDMRs, which was in line with the change in H3K27ac (Fig. 2F).

To further examine the effect of neuronal activity-dependent *de novo* DNA methylation on gene expression, we performed RNA-seq analyses of primary cultured mouse hippocampal neurons that were treated with either TTX or for 3 h with Bic/4AP. We linked the closest gene with a hyperDMR, regardless of the distance, using GREAT software (see *Materials and Methods*). We found that Bic/4AP-mediated neuronal hyperactivation decreased the expression of genes located near hyperDMRs (Fig. 2G-H). Gene ontology analysis for DMR-associated genes showed over-represented terms, such as nervous system development (Supplementary Fig. 5). Conversely, almost no change was observed in DNA methylation in regions where histone acetylation changed upon neuronal stimulation (Supplementary Fig. 6).

DNMT inhibitor inhibited neuronal activity-dependent excitatory synaptogenesis

To gain insight into the potential role of neuronal activity-dependent *de novo* DNA methylation, we examined synaptogenesis in neuronal

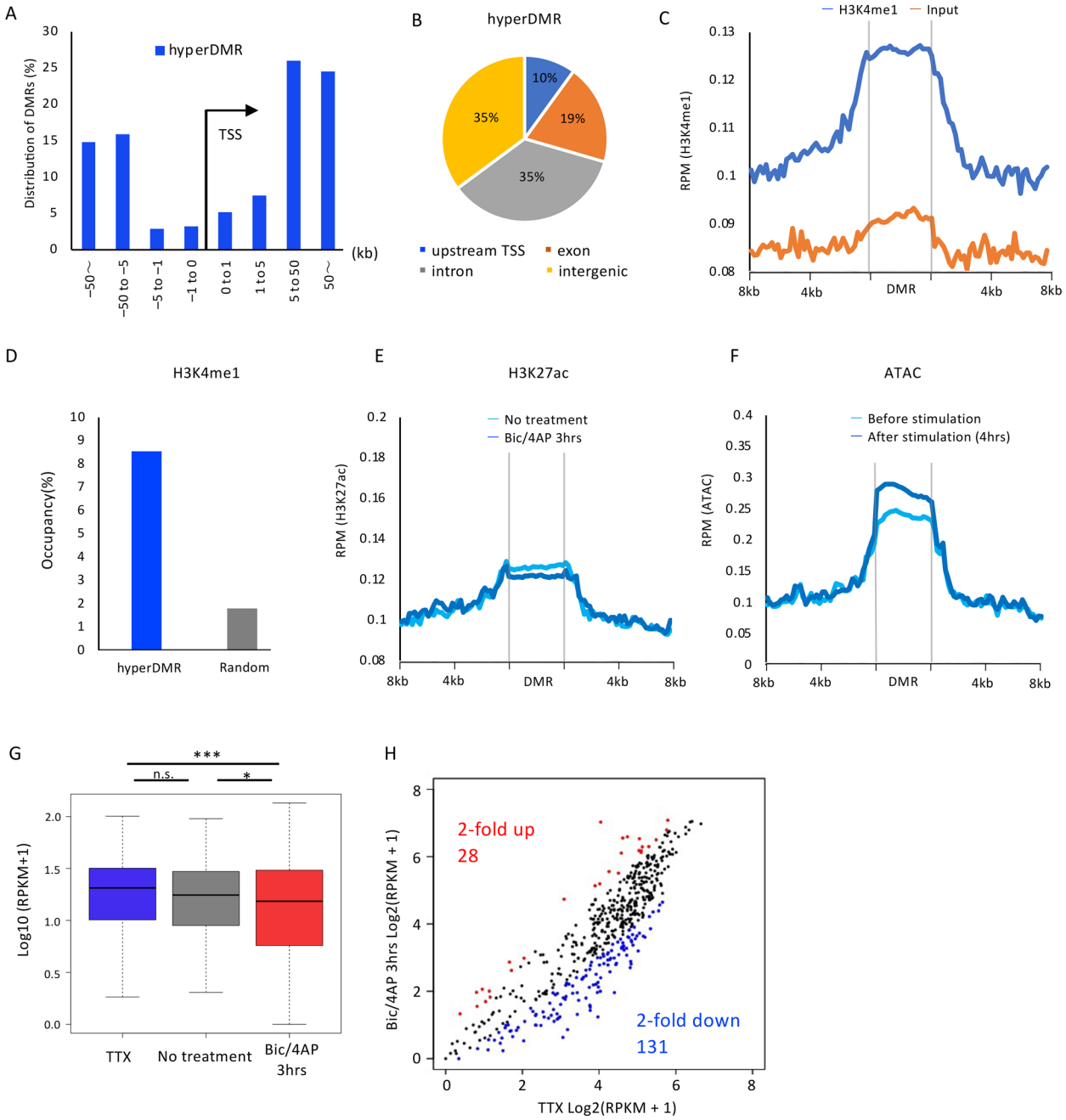

Fig. 2. Characteristics of hyperDMRs and relationship between DNA methylation and gene expression change. (A) Distribution of distance between hyperDMR and TSS. (B) Genomic locations of hyperDMRs in relation to the gene structure (upstream TSS: within 5 kb upstream from the TSS). (C) Enrichment profile of H3K4me1 around hyperDMRs. (D) Occupancy of H3K4me1 peaks in hyperDMRs (n = 826) or random regions (n = 800). (E) Enrichment profile of H3K27ac around hyperDMRs before neuronal activation and 3 h after Bic/4AP treatment. (F) Enrichment profile of ATAC-seq signal of adult mice dentate gyrus, before and after synchronous neuronal activation *via* electroconvulsive stimulation (GEO accession number: GSE82015) around hyperDMRs. (G) Boxplot of expression of hyperDMR-annotated genes in TTX-treated, untreated, and Bic/4AP-treated (for 3 h) samples. Average expressions of the triplicates are plotted. HyperDMRs were annotated to single nearest genes using GREAT software. n = 532, *** $P < 0.001$, * $P < 0.05$, n.s.: not significant, Mann–Whitney U test. (H) Scatter plot of expression of hyperDMR-associated genes between TTX-treated and Bic/4AP-treated (for 3 h) samples. Average expressions of the triplicates are plotted. Statistically significant 2-fold up- (red) and 2-fold down-regulated (blue) genes are highlighted. $P < 0.05$, Student's *t*-test.

preparations pre-treated with RG108, a well-known DNMT inhibitor, after Bic/4AP-induced neuronal activation. Immunocytochemical analysis of the RG108 (–) control showed that neuronal activation increased excitatory synapses, consistent with previous reports [53]. VGLUT1 is an excitatory presynaptic marker, and PSD95 is a post-synaptic marker; their co-localization indicates that they form excitatory synapses. In contrast, there was no increase in synaptic formation in the presence of RG108 (Fig. 3A-B). This indicated that global DNA methylation maintenance and/or induction mediated neuronal activity-dependent synaptogenesis. These results suggested that DNMT inhibitors affect the synaptic plasticity induced by neuronal activation.

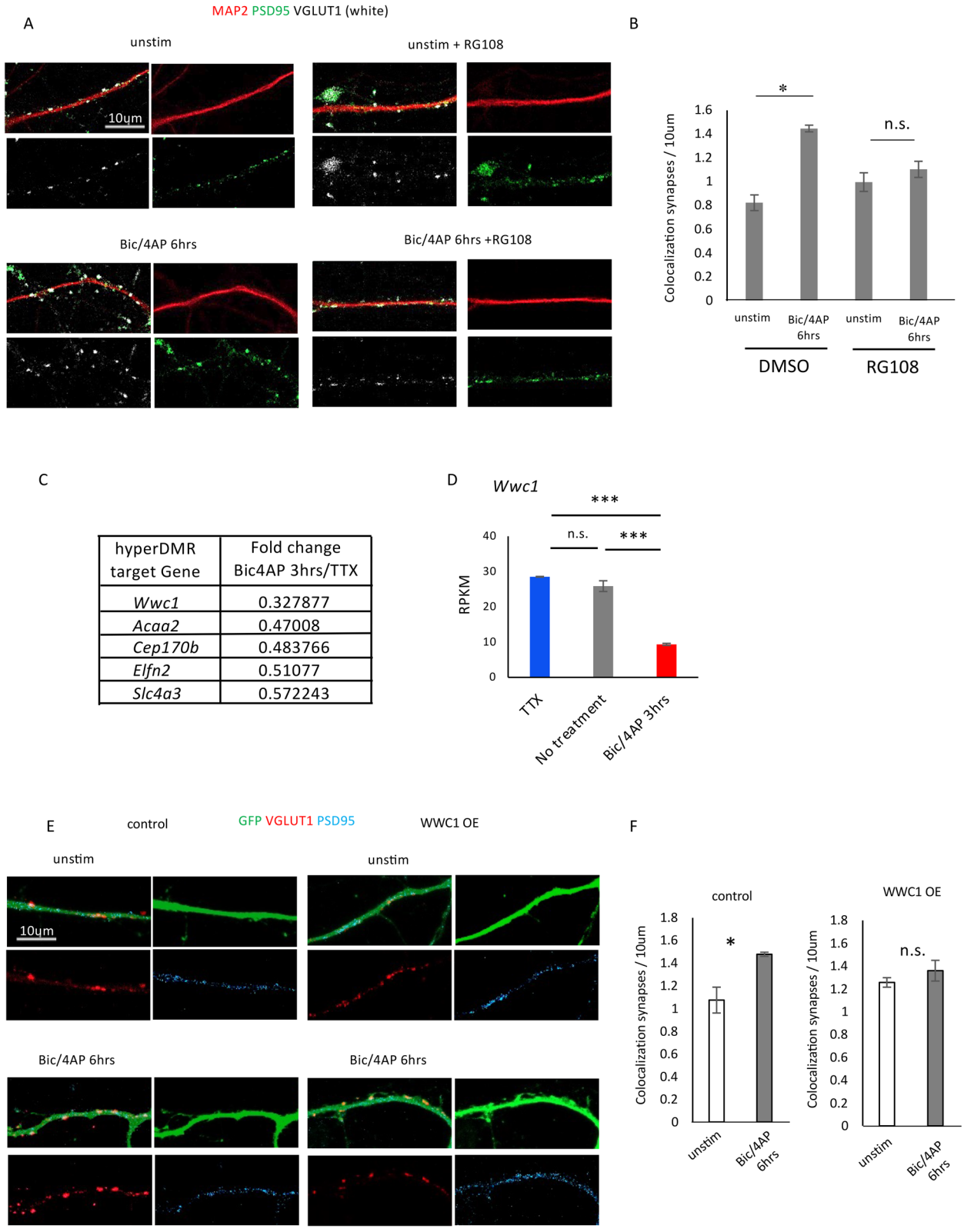

hyperDMR target Gene	Fold change Bic4AP 3hrs/TTX
Wwc1	0.327877
Acaa2	0.47008
Cep170b	0.483766
Elfn2	0.51077
Slc4a3	0.572243

Fig. 3. Effects of *de novo* DNA methylation on synaptogenesis. (A) Representative images of cultured hippocampal neurons stained with antibodies against VGLUT1, PSD-95, and MAP2. Scale bar: 10 μm. (B) Quantification of co-localized VGLUT1 and PSD-95 signals in (A) were quantified (n = 3, 10 neurons per replicate) * $P < 0.05$, n.s.: not significant, Student's *t*-test. (C) List of the Top 5 target genes for hyperDMR showing greatest downregulation during neuronal activation [methylation change ≥ 30%, highly expressed before Bic/4AP treatment (RPKM ≥ 25)]. (D) Expression levels of *Wwc1*. n = 3, *** $P < 0.001$, n.s.: not significant, Tukey–Kramer test. (E) Representative images of cultured hippocampal neurons stained with antibodies against VGLUT1, PSD-95, and GFP. Scale bar: 10 μm. (F) Quantification of co-localized VGLUT1 and PSD-95 signals in (E) (n = 3, 10 neurons per replicate) * $P < 0.05$, n.s.: not significant, Student's *t*-test.

Expression level of Wwc1 affected neuronal activity-dependent excitatory synaptogenesis

In order to obtain insight into the candidate target genes responsible for *de novo* DNA methylation-mediated neuronal activity-dependent synaptogenesis, we chose hyperDMR-partnered genes (hyperDMR ≥ 30%) that were highly expressed before Bic/4AP treatment (RPKM ≥ 25) and ranked them according to the degree of decrease in their gene expression upon neuronal activation. *Wwc1* was the most highly ranked among them (Fig. 3C-D). *Wwc1* is known to be involved in memory formation, synaptic plasticity, and neuronal morphology. It has also been reported that too much or too little expression of *Wwc1* affects neuronal morphology or synapse formation [54–56]. We hypothesized that *de novo* methylation of the *Wwc1* hyperDMR is important for activity-induced synaptogenesis. Therefore, we first performed overexpression experiments of *Wwc1* using lentivirus and examined synapse formation. Wwc1 did not appear to decrease synapse density. We postulated that *Wwc1* was already fully expressed before the stimulation, and therefore, overexpression had almost no effect on the basal condition. Interestingly, similar to the case of RG108-treated neurons, overexpression of *Wwc1* inhibited neuronal activity-dependent synapse formation (Fig. 3E-F). Furthermore, knockdown of *Wwc1* enhanced synaptogenesis (Supplementary Fig. 7). This presents the possibility that *Wwc1* is among the major target genes for *de novo* methylation-mediated neuronal activity-dependent synapse formation.

De novo DNA methylation regulated enhancer activity

To test the possibility that DNA methylation of the enhancer region of *Wwc1* and other candidates downregulates the corresponding genes, we examined the enhancer activity of select hyperDMRs using a reporter assay system with a CpG-free luciferase gene. First, we focused on the *Wwc1* hyperDMR. We confirmed that H3K4me1 accumulated in this hyperDMR (Fig. 4A-B). We then inserted the DNA fragment corresponding to this hyperDMR upstream of the hEF1 promoter in the CpG-free vector (Fig. 4C). After DNA methylation by M.Sss1 (a CpG methylase) (Fig. 4D), the test vector was transfected into retinoic acid-treated Neuro2a cells, a model system for investigating neuronal cell function, or E17 mouse hippocampal neurons. In this experimental setup, the promoter and luciferase were not targeted by DNA methylation and the expression was specifically affected by DNA methylation of the *Wwc1* hyperDMR. The results clearly showed that the *Wwc1* hyperDMR had enhancer activity, which was dramatically inactivated by DNA methylation (Fig. 4E-F). Similar results were obtained when the hyperDMRs located in the gene bodies of three genes [*Dpf1* (also known as *NeuroD4)*, *Kat6B*, and *Sergef*] were tested in this enhancer assay (Supplementary Fig. 8). Thus, we concluded that the hyperDMRs we discovered are enhancers that are silenced by *de novo* DNA methylation upon neuronal stimulation.

DNMT inhibitor inhibited neuronal activity-dependent de novo DNA methylation and affected gene expression

To further examine whether the DNMTs were responsible for neuronal activity-dependent *de novo* DNA methylation at the selected locus, we applied a DNMT inhibitor, RG108, before induction of neuronal activity. We then collected the sample 3 h after neuronal stimulation and subjected it to bisulfite sequencing. The data showed that there was impaired *de novo* DNA methylation in the *Wwc1* hyperDMR (Fig. 5A). As controls, we also analyzed the DNA methylation level of RG108-treated samples before neuronal activation and found no significant changes after this treatment (Supplementary Fig. 9A). In line with this impairment of DNA methylation, there was a significant increase in gene expression (Fig. 5B). This suggested that DNMTs may be involved in the neuronal activity-dependent *de novo* methylation of *Wwc1* enhancer, to prevent leaky expression of the corresponding gene.

Both DNMT1 and DNMT3a were involved in neuronal activity-dependent de novo DNA methylation

Finally, using lentivirus-expressing shRNA, a knockdown experiment was performed to determine which DNMT(s) contribute to *de novo* DNA methylation. Our RNA-seq data showed that DNMT1 and DNMT3a were highly expressed in primary cultured hippocampal neurons (Fig. 5C), and thus, we decided to target these genes (Supplementary Fig. 9B). No effects were observed upon knockdown of each gene alone. In contrast, upon simultaneous knockdown of both *Dnmt1* and *Dnmt3a*, a significant decrease in methylation was observed (Fig. 5D). Such epigenetic changes inhibited activity-dependent synaptogenesis, as was the case with RG108 treatment (Fig. 5E-F). These data indicated that the combinatorial effects of DNMT1 and DNMT3a are necessary for neuronal activity-dependent *de novo* DNA methylation.

Discussion

Previous studies using DNMT inhibitor-treated cells or DNMT knockout mice showed that enhancement of DNA demethylation due to the inability to maintain DNA methylation leads to disorders of synaptic plasticity, memory, and learning [15–17]. However, it should be noted that in addition to enhanced DNA demethylation, *de novo* DNA methylation should have been simultaneously impaired in those studies. Nevertheless, the functional significance of *de novo* DNA methylation dependent on neuronal activation has received little attention.

Therefore, we first investigated the epigenetic effects after neuronal activation in primary cultured hippocampal neurons and carefully checked the DNA methylation dynamics at single-base resolution. We clearly observed *de novo* DNA methylation and DNA demethylation in a genome-wide manner (Fig. 1A-B). While previous reports focused on DNA methylation changes near the promoter region, we found that enhancer regions were also targeted, and many hyperDMRs were located distal to the gene promoters (Fig. 2A). RNA-seq analysis revealed that methylation of hyperDMRs and gene expression were inversely correlated (Fig. 2F), supporting the idea that *de novo* DNA methylation of the enhancer regions may contribute to neuronal activity-dependent gene suppression.

Interestingly, we found that the regulation of enhancer activity by DNA methylation was not accompanied by a change in histone acetylation (Figs. 2E, 4A, Supplementary Fig. 8). So far, the regulation of enhancer activity has been explained in terms of increasing or decreasing histone acetylation [21, 22]. Although we did not examine histone acetylation after inhibition of DNMT activity, histone acetylation changes were not observed upon neuronal activation at *Kat6B* and *Sergef*, as well as, *Wwc1* (Fig. 4A, Supplementary Fig. 8). It is possible that neuronal activity-dependent *de novo* DNA methylation targets the enhancer regions to regulate gene expression, by physically reducing the binding of nuclear proteins to DNA, independent of the histone acetylation change. Our data highlight the importance of enhancer suppression by DNA methylation, without a change in histone acetylation, for neuronal activity-dependent gene silencing (Supplementary Fig. 6).

Inhibition of DNMT activity has been shown to regulate neuronal

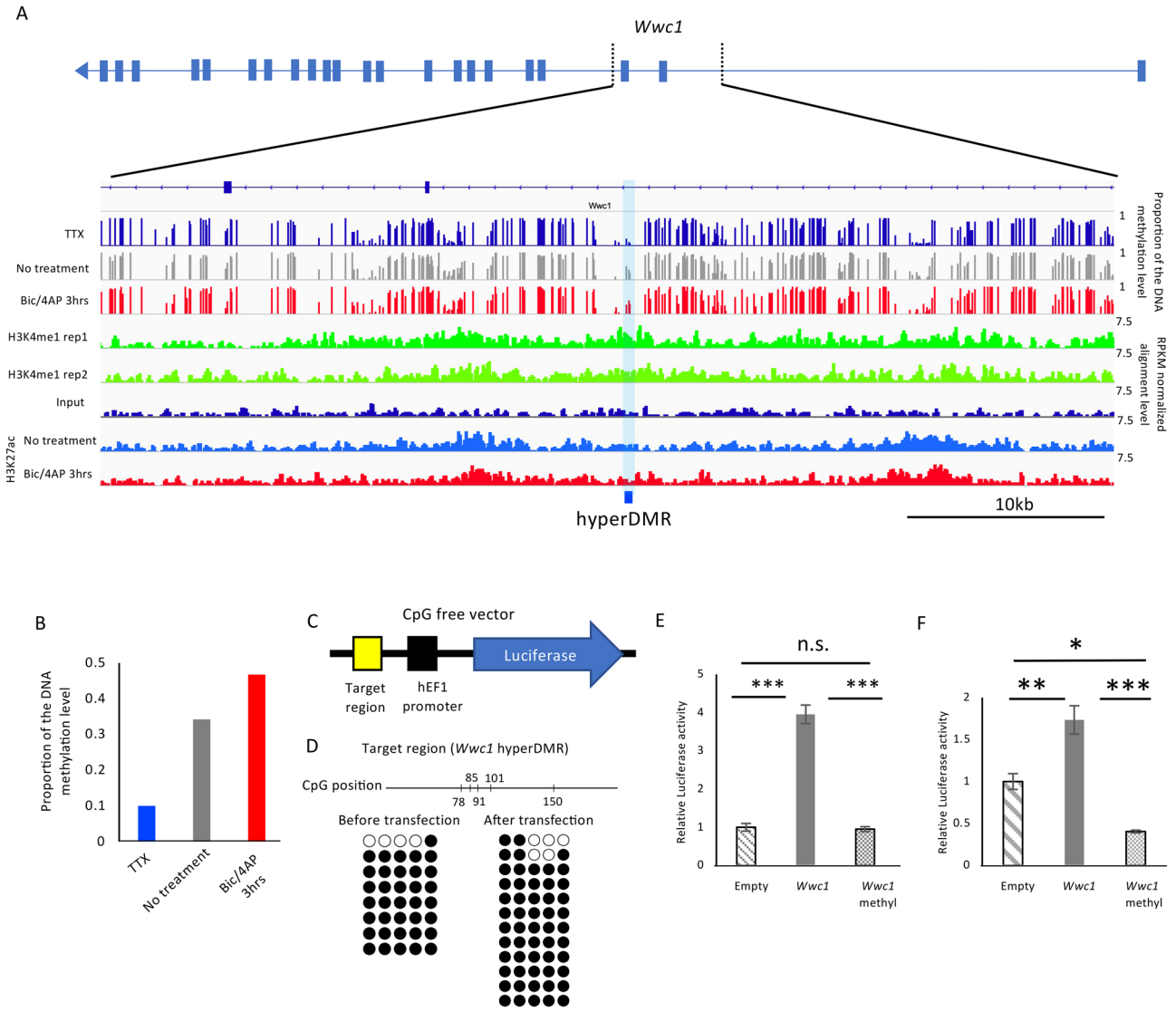

Fig. 4. Effect of DNA methylation on the enhancer region. (A) Alignment of WGBS, H3K4me1, and input around the hyperDMR at the *Wwc1* gene body. (B) DNA methylation level at the *Wwc1* hyperDMR from WGBS. (C) Structure of the CpG-free vector. (D) Bisulfite sequencing of the *Wwc1* hyperDMR inserted into the CpG-free vector after treatment with Sss1 methylase. Left and right panels correspond to the DNA methylation pattern before and after transfection, respectively. (E and F) Results of luciferase assay for empty, *Wwc1* hyperDMR, and methylated *Wwc1* hyperDMR using (E) Neuro2a differentiated into neuronal cells by retinoic acid treatment or (F) primary cultured hippocampal neurons. n = 4, * $P < 0.05$, ** $P < 0.01$, *** $P < 0.001$, n.s.: not significant, Tukey–Kramer test.

glutamatergic synaptic scaling and intrinsic membrane excitability [15, 16]. These studies noted a constant function of DNMTs, independent of neuronal activity. In the present study, the neuronal activity-dependent function of DNMTs was carefully assessed. We suppressed DNMT activity before the induction of neuronal activation, and then examined the effects of this suppression on activity-dependent neuronal physiology. Our results showed that inhibition of DNMTs inhibits synapse formation after neuronal activation (Fig. 3A-B), and downregulation of *Wwc1,* which is a hyperDMR target gene, contributes to this phenomenon (Fig. 3D-F). Neuronal activity-dependent physiological functions in neurons have been reported for immediate early response genes, including *Bdnf* and *Fos* [7, 21]. In contrast, the physiological functions of gene silencing in neurons are mostly unknown. In this context, our results are the first to demonstrate that DNMT activity during neuronal activation, leading to target gene repression through *de novo* DNA methylation at enhancer regions, plays important roles in synapse formation (Figs. 3, 4).

Recently, DNMT1 has been considered to be a maintenance methylation enzyme, while DNMT3a has been considered to be a *de novo* methylation enzyme. However, DNMT1 is also known to have *de novo* methylation activity [24, 25, 35, 36]. Our study showed that knockdown of either one of these enzymes alone had no effect on DNA methylation (Fig. 5D). However, it is known that double knockout of DNMT1 and DNMT3a affects memory and learning in adult mice [17], and our data support the idea that concomitant activity of both the DNMTs is important. We found that double knockdown of both DNMT1 and DNMT3a reduced DNA methylation (Fig. 5D). Previous double-knockouts focused on enhancing DNA demethylation, but based on the present findings, we can clearly say that both DNMT1 and DNMT3a are important for neuronal physiology through *de novo* DNA methylation. Since

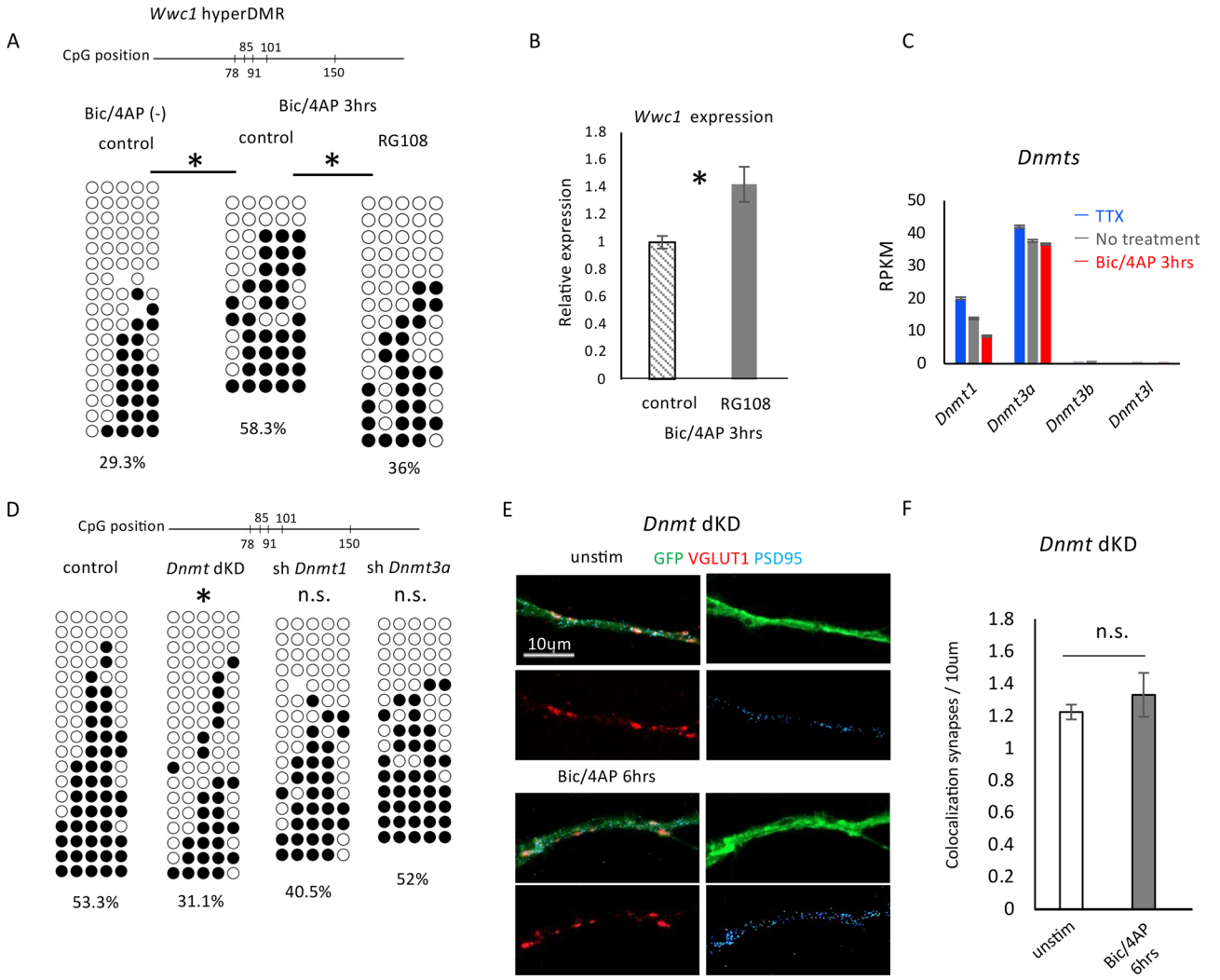

Fig. 5. Involvement of DNMTs in neuronal activity-dependent *de novo* DNA methylation. (A) Bisulfite sequencing of the hyperDMR located in the *Wwc1* gene body in cells treated with DMSO or RG108 before (DMSO) and 3 h after Bic/4AP treatment (DMSO or RG108). n = 3, * P < 0.05, Mann–Whitney U Test. (B) qRT-PCR analysis of *Wwc1* treated with DMSO or RG108, 3 h after Bic/4AP treatment. n = 3, * P < 0.05, Student's *t*-test. (C) Expression level of *Dnmts*, as analyzed using from RNA-seq data (n = 3). (D) Bisulfite sequencing of the hyperDMR located in the *Wwc1* gene body in cells expressing sh*Dnmt1* or/and sh*Dnmt3a* carried by lentivirus, 3 h after Bic/4AP treatment. n = 3, * P < 0.05, n.s.: not significant, Mann–Whitney U Test. (E) Representative images of cultured hippocampal neurons stained with antibodies against VGLUT1, PSD-95, and GFP. Scale bar: 10 μm. (F) Quantification of co-localized VGLUT1 and PSD-95 signals in (E) (n = 3, 10 neurons per replicate), n.s.: not significant, Student's *t*-test.

non-proliferating neurons may require little maintenance methylation compared to proliferating cells, DNMT1 and DNMT3a might play a role in *de novo* DNA methylation in neurons. Considering the establishment of DNA methylation in reproductive machinery, the requirements of DNMT1 and DNMT3a in the establishment of neuronal DNA methylation highlight the importance of this study. In fact, highly dynamic CpG and non-CpG methylation have been observed in mouse oocytes. For example, after a short *in vitro* culture of freshly ovulated oocytes, *Peg1/Mest,* a well-known imprinted gene, becomes hypermethylated, whereas prolonged *in vitro* culture results in demethylation in a fraction of oocytes [57]. Previous studies have shown that DNMT3a and DNMT3l, but not DNMT1, are involved in *de novo* DNA methylation in oocytes, even after cell cycle exit [58]. It is most likely that all DNMTs have specific functions in the formation of DNA methylation patterns during different stages of development. Therefore, our findings on *de novo* DNA methylation will also have considerable implications for the understanding of epigenetic regulation in the formation of germ cells, fertilized embryos, and fetuses.

Our findings would have broad implications for understanding the epigenetic regulation of the nervous system under physiological and pathological conditions, in line with the findings of a recent publication, which showed that *de novo* DNA methylation at enhancers inactivates enhancer activity during neural maturation [59]. Since DNA methylation defects are a cause of autism spectrum disorder or intellectual disabilities [60, 61], identifying genomic loci that undergo dynamic changes in DNA methylation may provide ways to cure such disorders/disabilities through targeted epigenome editing. This study clearly showed that the DNA methylation system plays a fundamental role in the functioning of terminally differentiated cells, in addition to the formation, proliferation, and differentiation of tissue stem cells. For example, our findings strongly suggest that DNA methylation in many post-mitotic cells may be affected by changes in the maternal environment. In this context, further

investigation of functional targets, including *Wwc1*, will lead to a new trend in reproductive biology.

Our results identified neuronal activity-induced *de novo* DNA methylation as a regulator of enhancer activity that affects excitatory synaptogenesis. Therefore, *de novo* DNA methylation has a much broader and more fundamental role in neurons than previously recognized. Although studies of neuronal activity-induced DNA methylation have traditionally focused on its roles in the regulation of promoter activity [7, 9], our results suggest a previously underappreciated role for *de novo* DNA methylation in the regulation of enhancer activity.

Availability of data and materials: The datasets generated and analyzed during the current study are available in the NCBI Gene Expression Omnibus repository under accession number GSE149342 (https://www.ncbi.nlm.nih.gov/geo/query/acc.cgi?acc=GSE149342). The datasets used and analyzed during the current study are available in the NCBI Gene Expression Omnibus repository under accession numbers GSE21161 (https://www.ncbi.nlm.nih.gov/geo/query/acc.cgi?acc=GSE21161) and GSE82015 (https://www.ncbi.nlm.nih.gov/geo/query/acc.cgi?acc=GSE82015).

Conflict of interests: The authors have nothing to declare.

Acknowledgements

We appreciate the technical assistance from The Research Support Center, Research Center for Human Disease Modeling, Kyushu University Graduate School of Medical Sciences. We thank S. Katada and T. Matsuda for their experimental advice, Y. Nakagawa for her excellent secretarial assistance, and Elizabeth Nakajima for proofreading the manuscript. We thank Dr. H. Kimura (Tokyo Institute of Technology) for sharing the histone H3K27ac and H3K4me1 antibodies.

This work was supported by JSPS KAKENHI [grant numbers 15H04603 and 19H03138 to T. Imamura, 16H06279 (PAGS)], the Platform Project for Supporting Drug Discovery and Life Science Research (Platform for Drug Discovery, Informatics, and Structural Life Science) from the Japan Agency for Medical Research and Development (AMED), Platform Project for Supporting Drug Discovery and Life Science Research [Basis for Supporting Innovative Drug Discovery and Life Science Research (BINDS)] from AMED [grant number JP20am0101103], the Research Program of Innovative Cell Biology by Innovative Technology (Cell Innovation), Grant-in-Aid for JSPS Fellows [18J21142 to TK], MEXT Grant-in-Aid for Scientific Research on Innovative Areas [16H06527 to KN], and grants from Takeda Science Foundation and Uehara Memorial Foundation to T Imamura.

References

1. **Chen L, MacMillan AM, Chang W, Ezaz-Nikpay K, Lane WS, Verdine GL.** Direct identification of the active-site nucleophile in a DNA (cytosine-5)-methyltransferase. *Biochemistry* 1991; **30**: 11018–11025. [Medline] [CrossRef]
2. **Moore LD, Le T, Fan G.** DNA methylation and its basic function. *Neuropsychopharmacology* 2013; **38**: 23–38. [Medline] [CrossRef]
3. **Bird A.** DNA methylation patterns and epigenetic memory. *Genes Dev* 2002; **16**: 6–21. [Medline] [CrossRef]
4. **Law JA, Jacobsen SE.** Establishing, maintaining and modifying DNA methylation patterns in plants and animals. *Nat Rev Genet* 2010; **11**: 204–220. [Medline] [CrossRef]
5. **Sanosaka T, Imamura T, Hamazaki N, Chai M, Igarashi K, Ideta-Otsuka M, Miura F, Ito T, Fujii N, Ikeo K, Nakashima K.** DNA methylome analysis identifies transcription factor-based epigenomic signatures of multilineage competence in neural stem/progenitor cells. *Cell Reports* 2017; **20**: 2992–3003. [Medline] [CrossRef]
6. **Gräff J, Kim D, Dobbin MM, Tsai LH.** Epigenetic regulation of gene expression in physiological and pathological brain processes. *Physiol Rev* 2011; **91**: 603–649. [Medline] [CrossRef]
7. **Yu H, Su Y, Shin J, Zhong C, Guo JU, Weng YL, Gao F, Geschwind DH, Coppola G, Ming GL, Song H.** Tet3 regulates synaptic transmission and homeostatic plasticity via DNA oxidation and repair. *Nat Neurosci* 2015; **18**: 836–843. [Medline] [CrossRef]
8. **Martinowich K, Hattori D, Wu H, Fouse S, He F, Hu Y, Fan G, Sun YE.** DNA methylation-related chromatin remodeling in activity-dependent BDNF gene regulation. *Science* 2003; **302**: 890–893. [Medline] [CrossRef]
9. **Miller CA, Sweatt JD.** Covalent modification of DNA regulates memory formation. *Neuron* 2007; **53**: 857–869. [Medline] [CrossRef]
10. **Nelson ED, Kavalali ET, Monteggia LM.** Activity-dependent suppression of miniature neurotransmission through the regulation of DNA methylation. *J Neurosci* 2008; **28**: 395–406. [Medline] [CrossRef]
11. **Ma DK, Jang MH, Guo JU, Kitabatake Y, Chang ML, Pow-Anpongkul N, Flavell RA, Lu B, Ming GL, Song H.** Neuronal activity-induced Gadd45b promotes epigenetic DNA demethylation and adult neurogenesis. *Science* 2009; **323**: 1074–1077. [Medline] [CrossRef]
12. **Guo JU, Su Y, Zhong C, Ming GL, Song H.** Hydroxylation of 5-methylcytosine by TET1 promotes active DNA demethylation in the adult brain. *Cell* 2011; **145**: 423–434. [Medline] [CrossRef]
13. **Guo JU, Ma DK, Mo H, Ball MP, Jang MH, Bonaguidi MA, Balazer JA, Eaves HL, Xie B, Ford E, Zhang K, Ming GL, Gao Y, Song H.** Neuronal activity modifies the DNA methylation landscape in the adult brain. *Nat Neurosci* 2011; **14**: 1345–1351. [Medline] [CrossRef]
14. **Maddox SA, Watts CS, Schafe GE.** DNA methyltransferase activity is required for memory-related neural plasticity in the lateral amygdala. *Neurobiol Learn Mem* 2014; **107**: 93–100. [Medline] [CrossRef]
15. **Meadows JP, Guzman-Karlsson MC, Phillips S, Brown JA, Strange SK, Sweatt JD, Hablitz JJ.** Dynamic DNA methylation regulates neuronal intrinsic membrane excitability. *Sci Signal* 2016; **9**: ra83. [Medline] [CrossRef]
16. **Meadows JP, Guzman-Karlsson MC, Phillips S, Holleman C, Posey JL, Day JJ, Hablitz JJ, Sweatt JD.** DNA methylation regulates neuronal glutamatergic synaptic scaling. *Sci Signal* 2015; **8**: ra61. [Medline] [CrossRef]
17. **Feng J, Zhou Y, Campbell SL, Le T, Li E, Sweatt JD, Silva AJ, Fan G.** Dnmt1 and Dnmt3a maintain DNA methylation and regulate synaptic function in adult forebrain neurons. *Nat Neurosci* 2010; **13**: 423–430. [Medline] [CrossRef]
18. **Halder R, Hennion M, Vidal RO, Shomroni O, Rahman RU, Rajput A, Centeno TP, van Bebber F, Capece V, Garcia Vizcaino JC, Schuetz AL, Burkhardt S, Benito E, Navarro Sala M, Javan SB, Haass C, Schmid B, Fischer A, Bonn S.** DNA methylation changes in plasticity genes accompany the formation and maintenance of memory. *Nat Neurosci* 2016; **19**: 102–110. [Medline] [CrossRef]
19. **Peixoto L, Abel T.** The role of histone acetylation in memory formation and cognitive impairments. *Neuropsychopharmacology* 2013; **38**: 62–76. [Medline] [CrossRef]
20. **Levenson JM, O'Riordan KJ, Brown KD, Trinh MA, Molfese DL, Sweatt JD.** Regulation of histone acetylation during memory formation in the hippocampus. *J Biol Chem* 2004; **279**: 40545–40559. [Medline] [CrossRef]
21. **Malik AN, Vierbuchen T, Hemberg M, Rubin AA, Ling E, Couch CH, Stroud H, Spiegel I, Farh KK, Harmin DA, Greenberg ME.** Genome-wide identification and characterization of functional neuronal activity-dependent enhancers. *Nat Neurosci* 2014; **17**: 1330–1339. [Medline] [CrossRef]
22. **Kim TK, Hemberg M, Gray JM, Costa AM, Bear DM, Wu J, Harmin DA, Laptewicz M, Barbara-Haley K, Kuersten S, Markenscoff-Papadimitriou E, Kuhl D, Bito H, Worley PF, Kreiman G, Greenberg ME.** Widespread transcription at neuronal activity-regulated enhancers. *Nature* 2010; **465**: 182–187. [Medline] [CrossRef]
23. **Sun Z, Xu X, He J, Murray A, Sun MA, Wei X, Wang X, McCoig E, Xie E, Jiang X, Li L, Zhu J, Chen J, Morozov A, Pickrell AM, Theus MH, Xie H.** EGR1 recruits TET1 to shape the brain methylome during development and upon neuronal activity. *Nat Commun* 2019; **10**: 3892. [Medline] [CrossRef]
24. **Goto K, Numata M, Komura JI, Ono T, Bestor TH, Kondo H.** Expression of DNA methyltransferase gene in mature and immature neurons as well as proliferating cells in mice. *Differentiation* 1994; **56**: 39–44. [Medline] [CrossRef]
25. **Inano K, Suetake I, Ueda T, Miyake Y, Nakamura M, Okada M, Tajima S.** Maintenance-type DNA methyltransferase is highly expressed in post-mitotic neurons and localized in the cytoplasmic compartment. *J Biochem* 2000; **128**: 315–321. [Medline] [CrossRef]
26. **Miller CA, Campbell SL, Sweatt JD.** DNA methylation and histone acetylation work in concert to regulate memory formation and synaptic plasticity. *Neurobiol Learn Mem* 2008; **89**: 599–603. [Medline] [CrossRef]
27. **Aapola U, Kawasaki K, Scott HS, Ollila J, Vihinen M, Heino M, Shintani A, Kawasaki K, Minoshima S, Krohn K, Antonarakis SE, Shimizu N, Kudoh J, Peterson P.** Isolation and initial characterization of a novel zinc finger gene, DNMT3L, on 21q22.3, related to the cytosine-5-methyltransferase 3 gene family. *Genomics* 2000; **65**: 293–298. [Medline] [CrossRef]
28. **Aapola U, Lyle R, Krohn K, Antonarakis SE, Peterson P.** Isolation and initial characterization of the mouse Dnmt3l gene. *Cytogenet Cell Genet* 2001; **92**: 122–126. [Medline] [CrossRef]

29. **Bourc'his D, Xu GL, Lin CS, Bollman B, Bestor TH.** Dnmt3L and the establishment of maternal genomic imprints. *Science* 2001; **294**: 2536–2539. [Medline] [CrossRef]
30. **Chedin F, Lieber MR, Hsieh CL.** The DNA methyltransferase-like protein DNMT3L stimulates de novo methylation by Dnmt3a. *Proc Natl Acad Sci USA* 2002; **99**: 16916–16921. [Medline] [CrossRef]
31. **Bourc'his D, Bestor TH.** Meiotic catastrophe and retrotransposon reactivation in male germ cells lacking Dnmt3L. *Nature* 2004; **431**: 96–99. [Medline] [CrossRef]
32. **Suetake I, Shinozaki F, Miyagawa J, Takeshima H, Tajima S.** DNMT3L stimulates the DNA methylation activity of Dnmt3a and Dnmt3b through a direct interaction. *J Biol Chem* 2004; **279**: 27816–27823. [Medline] [CrossRef]
33. **Holz-Schietinger C, Reich NO.** The inherent processivity of the human de novo methyltransferase 3A (DNMT3A) is enhanced by DNMT3L. *J Biol Chem* 2010; **285**: 29091–29100. [Medline] [CrossRef]
34. **Ichiyanagi T, Ichiyanagi K, Miyake M, Sasaki H.** Accumulation and loss of asymmetric non-CpG methylation during male germ-cell development. *Nucleic Acids Res* 2013; **41**: 738–745. [Medline] [CrossRef]
35. **Yarychkivska O, Shahabuddin Z, Comfort N, Boulard M, Bestor TH.** BAH domains and a histone-like motif in DNA methyltransferase 1 (DNMT1) regulate *de novo* and maintenance methylation *in vivo*. *J Biol Chem* 2018; **293**: 19466–19475. [Medline] [CrossRef]
36. **Fatemi M, Hermann A, Gowher H, Jeltsch A.** Dnmt3a and Dnmt1 functionally cooperate during de novo methylation of DNA. *Eur J Biochem* 2002; **269**: 4981–4984. [Medline] [CrossRef]
37. **Li Y, Zhang Z, Chen J, Liu W, Lai W, Liu B, Li X, Liu L, Xu S, Dong Q, Wang M, Duan X, Tan J, Zheng Y, Zhang P, Fan G, Wong J, Xu GL, Wang Z, Wang H, Gao S, Zhu B.** Stella safeguards the oocyte methylome by preventing de novo methylation mediated by DNMT1. *Nature* 2018; **564**: 136–140. [Medline] [CrossRef]
38. **Lois C, Hong EJ, Pease S, Brown EJ, Baltimore D.** Germline transmission and tissue-specific expression of transgenes delivered by lentiviral vectors. *Science* 2002; **295**: 868–872. [Medline] [CrossRef]
39. **Zhou Z, Hong EJ, Cohen S, Zhao WN, Ho HY, Schmidt L, Chen WG, Lin Y, Savner E, Griffith EC, Hu L, Steen JA, Weitz CJ, Greenberg ME.** Brain-specific phosphorylation of MeCP2 regulates activity-dependent Bdnf transcription, dendritic growth, and spine maturation. *Neuron* 2006; **52**: 255–269. [Medline] [CrossRef]
40. **Nakashima H, Tsujimura K, Irie K, Ishizu M, Pan M, Kameda T, Nakashima K.** Canonical TGF-β signaling negatively regulates neuronal morphogenesis through TGIF/Smad complex-mediated CRMP2 suppression. *J Neurosci* 2018; **38**: 4791–4810. [Medline] [CrossRef]
41. **Tsujimura K, Irie K, Nakashima H, Egashira Y, Fukao Y, Fujiwara M, Itoh M, Uesaka M, Imamura T, Nakahata Y, Yamashita Y, Abe T, Takamori S, Nakashima K.** miR-199a links MeCP2 with mTOR signaling and its dysregulation leads to rett syndrome phenotypes. *Cell Reports* 2015; **12**: 1887–1901. [Medline] [CrossRef]
42. **Hamazaki N, Uesaka M, Nakashima K, Agata K, Imamura T.** Gene activation-associated long noncoding RNAs function in mouse preimplantation development. *Development* 2015; **142**: 910–920. [Medline]
43. **Patel RK, Jain M.** NGS QC Toolkit: a toolkit for quality control of next generation sequencing data. *PLoS One* 2012; **7**: e30619. [Medline] [CrossRef]
44. **Kim D, Pertea G, Trapnell C, Pimentel H, Kelley R, Salzberg SL.** TopHat2: accurate alignment of transcriptomes in the presence of insertions, deletions and gene fusions. *Genome Biol* 2013; **14**: R36. [Medline] [CrossRef]
45. **Matsuda T, Irie T, Katsurabayashi S, Hayashi Y, Nagai T, Hamazaki N, Adefuin AMD, Miura F, Ito T, Kimura H, Shirahige K, Takeda T, Iwasaki K, Imamura T, Nakashima K.** Pioneer factor neurod1 rearranges transcriptional and epigenetic profiles to execute microglia-neuron conversion. *Neuron* 2019; **101**: 472–485.e7. [Medline] [CrossRef]
46. **Zhang Y, Liu T, Meyer CA, Eeckhoute J, Johnson DS, Bernstein BE, Nusbaum C, Myers RM, Brown M, Li W, Liu XS.** Model-based analysis of ChIP-Seq (MACS). *Genome Biol* 2008; **9**: R137. [Medline] [CrossRef]
47. **McLean CY, Bristor D, Hiller M, Clarke SL, Schaar BT, Lowe CB, Wenger AM, Bejerano G.** GREAT improves functional interpretation of cis-regulatory regions. *Nat Biotechnol* 2010; **28**: 495–501. [Medline] [CrossRef]
48. **Shen L, Shao N, Liu X, Nestler E.** ngs.plot: Quick mining and visualization of next-generation sequencing data by integrating genomic databases. *BMC Genomics* 2014; **15**: 284. [Medline] [CrossRef]
49. **Miura F, Enomoto Y, Dairiki R, Ito T.** Amplification-free whole-genome bisulfite sequencing by post-bisulfite adaptor tagging. *Nucleic Acids Res* 2012; **40**: e136. [Medline] [CrossRef]
50. **Miura F, Ito T.** Post-Bisulfite Adaptor Tagging for PCR-Free Whole-Genome Bisulfite Sequencing. *Methods Mol Biol* 2018; **1708**: 123–136. [Medline] [CrossRef]
51. **Huang W, Sherman BT, Lempicki RA.** Systematic and integrative analysis of large gene lists using DAVID bioinformatics resources. *Nat Protoc* 2009; **4**: 44–57. [Medline] [CrossRef]
52. **Su Y, Shin J, Zhong C, Wang S, Roychowdhury P, Lim J, Kim D, Ming GL, Song H.** Neuronal activity modifies the chromatin accessibility landscape in the adult brain. *Nat Neurosci* 2017; **20**: 476–483. [Medline] [CrossRef]
53. **Zito K, Svoboda K.** Activity-dependent synaptogenesis in the adult Mammalian cortex. *Neuron* 2002; **35**: 1015–1017. [Medline] [CrossRef]
54. **Williams AA, White R, Siniard A, Corneveaux J, Huentelman M, Duch C.** MECP2 impairs neuronal structure by regulating KIBRA. *Neurobiol Dis* 2016; **91**: 284–291. [Medline] [CrossRef]
55. **Blanque A, Repetto D, Rohlmann A, Brockhaus J, Duning K, Pavenstädt H, Wolff I, Missler M.** Deletion of KIBRA, protein expressed in kidney and brain, increases filopodial-like long dendritic spines in neocortical and hippocampal neurons in vivo and in vitro. *Front Neuroanat* 2015; **9**: 13. [Medline] [CrossRef]
56. **Ji Z, Li H, Yang Z, Huang X, Ke X, Ma S, Lin Z, Lu Y, Zhang M.** Kibra modulates learning and memory via binding to dendrin. *Cell Reports* 2019; **26**: 2064–2077.e7. [Medline] [CrossRef]
57. **Imamura T, Kerjean A, Heams T, Kupiec JJ, Thenevin C, Pàldi A.** Dynamic CpG and non-CpG methylation of the Peg1/Mest gene in the mouse oocyte and preimplantation embryo. *J Biol Chem* 2005; **280**: 20171–20175. [Medline] [CrossRef]
58. **Shirane K, Toh H, Kobayashi H, Miura F, Chiba H, Ito T, Kono T, Sasaki H.** Mouse oocyte methylomes at base resolution reveal genome-wide accumulation of non-CpG methylation and role of DNA methyltransferases. *PLoS Genet* 2013; **9**: e1003439. [Medline] [CrossRef]
59. **Stroud H, Yang MG, Tsitohay YN, Davis CP, Sherman MA, Hrvatin S, Ling E, Greenberg ME.** An activity-mediated transition in transcription in early postnatal neurons. *Neuron* 2020; **107**: 874–890.e8. [Medline] [CrossRef]
60. **Tatton-Brown K, Seal S, Ruark E, Harmer J, Ramsay E, Del Vecchio Duarte S, Zachariou A, Hanks S, O'Brien E, Aksglaede L, Baralle D, Dabir T, Gener B, Goudie D, Homfray T, Kumar A, Pilz DT, Selicorni A, Temple IK, Van Maldergem L, Yachelevich N, van Montfort R, Rahman N, Consortium CO. Childhood Overgrowth Consortium.** Mutations in the DNA methyltransferase gene DNMT3A cause an overgrowth syndrome with intellectual disability. *Nat Genet* 2014; **46**: 385–388. [Medline] [CrossRef]
61. **Sanders SJ, He X, Willsey AJ, Ercan-Sencicek AG, Samocha KE, Cicek AE, Murtha MT, Bal VH, Bishop SL, Dong S, Goldberg AP, Jinlu C, Keaney JF 3rd, Klei L, Mandell JD, Moreno-De-Luca D, Poultney CS, Robinson EB, Smith L, Solli-Nowlan T, Su MY, Teran NA, Walker MF, Werling DM, Beaudet AL, Cantor RM, Fombonne E, Geschwind DH, Grice DE, Lord C, Lowe JK, Mane SM, Martin DM, Morrow EM, Talkowski ME, Sutcliffe JS, Walsh CA, Yu TW, Ledbetter DH, Martin CL, Cook EH, Buxbaum JD, Daly MJ, Devlin B, Roeder K, State MW, Consortium AS. Autism Sequencing Consortium.** Insights into autism spectrum disorder genomic architecture and biology from 71 risk loci. *Neuron* 2015; **87**: 1215–1233. [Medline] [CrossRef]